OPEN

Mast cell-derived neurotrophin 4 mediates allergen-induced airway hyperinnervation in early life

KR Patel[1], L Aven[1], F Shao[1], N Krishnamoorthy[3], MG Duvall[2,3], BD Levy[3] and X Ai[1,3]

Asthma often progresses from early episodes of insults. How early-life events connect to long-term airway dysfunction remains poorly understood. We demonstrated previously that increased neurotrophin 4 (NT4) levels following early-life allergen exposure cause persistent changes in airway smooth muscle (ASM) innervation and airway hyper-reactivity (AHR) in mice. Herein, we identify pulmonary mast cells as a key source of aberrant NT4 expression following early insults. NT4 is selectively expressed by ASM and mast cells in mice, nonhuman primates, and humans. We show in mice that mast cell-derived NT4 is dispensable for ASM innervation during development. However, upon insults, mast cells expand in number and degranulate to release NT4 and thus become the major source of NT4 under pathological condition. Adoptive transfer of wild-type mast cells, but not *NT4*$^{-/-}$ mast cells restores ASM hyperinnervation and AHR in *Kit*$^{W\text{-}sh/W\text{-}sh}$ mice following early-life insults. Notably, an infant nonhuman primate model of asthma also exhibits ASM hyperinnervation associated with the expansion and degranulation of mast cells. Together, these findings identify an essential role of mast cells in mediating ASM hyperinnervation following early-life insults by producing NT4. This role may be evolutionarily conserved in linking early insults to long-term airway dysfunction.

INTRODUCTION

Asthma is a chronic respiratory disease that often progresses from childhood to adulthood.[1] Risk factors for asthma include early-life exposure to allergen, cigarette smoke, ozone (O_3), and respiratory viral infection. As the lung continues to grow after birth, environmental insults during infancy and early childhood may cause prolonged changes in lung structure, function, and disease susceptibility.[2–5] However, the mechanism that connects early events to long-term airway dysfunction remains poorly understood. As a direct consequence, treatment strategies that prevent asthma in young children at high risk are lacking.

Previous studies in rodents and nonhuman primates showed that the levels of neural innervation in immature lungs are prone to change by insults. Respiratory syncytial virus infection in neonatal guinea pigs increases peptidergic, sensory nerves in the lower airway.[6] Early-life exposure to O_3 or cigarette smoke in rats and mice similarly increases sensory and sympathetic innervation of the airway.[7] Employing a neonatal mouse model of ovalbumin (OVA) and cockroach allergen exposure, we showed that airway smooth muscle (ASM) hyperinnervation is functionally linked to persistent airway hyper-reactivity (AHR) into adulthood.[2] Furthermore, nonhuman primates exhibit changes in airway innervation following perinatal and neonatal exposure to O_3, house dust mite allergen (HDMA), or cigarette smoke.[8,9] In contrast, similar insults to mature adult lungs in animal models have little quantitative effect on airway innervation and elicit transient airway dysfunction.[2,10]

We showed in neonatal mice that allergen exposure elevates neurotrophin 4 (NT4) expression to induce ASM hyperinnervation.[2] NT4 belongs to a nerve growth factor family that has essential roles in the development of the nervous system.[11] During lung development, NT4 expressed by ASM serves as a target-derived neurotrophic factor for ASM innervation.[2] However, how NT4 expression is aberrantly upregulated following early-life allergen exposure is unknown. Consistent

[1]The Pulmonary Center, Department of Medicine, Boston University School of Medicine, Boston, Massachusetts, USA. [2]Division of Critical Care Medicine, Department of Anesthesia, Perioperative and Pain Medicine, Boston Children's Hospital, Boston, Massachusetts, USA and [3]Division of Pulmonary and Critical Care Medicine, Brigham & Women's Hospital, Harvard Medical School, Boston, Massachusetts, USA. Correspondence: X Ai (xai@partners.org)

Received 16 September 2015; accepted 4 January 2016; published online 10 February 2016. doi:10.1038/mi.2016.11

with a role of aberrant NT4 expression in long-term airway dysfunction in the neonatal mouse model, members of the NT family are overexpressed in lungs of infant nonhuman primates following exposure to cigarette smoke and in human infants who are infected with respiratory syncytial virus.[9,12] In addition, serum levels of NT4 are positively correlated with disease severity in children with asthma.[13] These findings suggest that NT overexpression and associated airway hyperinnervation may be evolutionarily conserved, early events that ultimately contribute to pathogenesis of asthma.

Mast cells are known to interact with nerves and these interactions have been implicated in several diseases, such as multiple sclerosis, interstitial cystitis, irritable bowel syndrome, and atopic dermatitis.[14] In the lung, mast cells are often found in intra-epithelial and intra-muscular spaces in close proximity to nerves.[15–17] The pulmonary mast cells are known to communicate with cholinergic nerves through serotonin secretion causing AHR in adult mice.[18,19] Peritoneal mast cells are also known to express NTs.[20] Whether mast cells contribute to changes in NT expression in neonatal mouse models of asthma and in childhood asthma is unknown.

In this study, we investigate how early-life allergen exposure in mice elevates the levels of NT4 to increase ASM innervation, which in turn causes AHR. This study is powered by parallel characterization of samples from mice, nonhuman primates, and humans followed by in-depth mechanistic studies using mouse genetics and functional rescue assays. Herein, we identify NT4 released from pulmonary mast cells as the underlying mechanism of allergen-induced ASM hyperinnervation in neonatal mice and provide evidence that this neuromodulatory role of mast cells may be conserved in primates.

RESULTS

Early-life insults lead to an increase in ASM innervation in nonhuman primates

We showed in a neonatal mouse model that allergen exposure elevates NT4 levels to increase ASM innervation.[2] NTs are also overexpressed in lungs of respiratory syncytial virus-infected infants and in severe childhood asthma,[12,13] yet their relationship to airway innervation in these young patients is unknown owing to technical difficulties of obtaining tissue samples. To address this issue, we assessed whether insults in infant rhesus monkeys increase ASM innervation using resources provided by California National Primate Research Center at University of California Davis (http://www.cnprc.ucdavis.edu/our-science/respiratory-diseases/). This infant nonhuman primate model of O_3 and HDMA exposure for 6 months after birth faithfully recapitulates the clinical hallmarks of asthma and disease progression (**Figure 1a**).[21] Proximal primate lung sections were double stained for neuron specific β-tubulin using a TuJ1 antibody and ASM using a smooth muscle actin (SMA) antibody (**Figure 1b**). Axon density was calculated by normalizing TuJ1 immunoreactivity to the SMA^+ area. Compared with filtered air-exposed controls, O_3 + HDMA exposure significantly increased ASM innervation by ~70% (**Figure 1c**). These findings indicate that early-life insults increase ASM innervation in nonhuman primates.

Mast cells are a candidate source of NT4 in neonatal mouse and nonhuman primate models of allergic asthma and in humans

Given the central role of elevated NT4 levels in ASM hyperinnervation and persistent AHR in the neonatal mouse model of allergen exposure, we set out to identify the cellular source of aberrant NT4 expression following early-life insults. We first assessed whether OVA exposure increased NT4 expression in ASM in mice. NT4 is expressed in ASM and serves as a target-derived neurotrophic factor for innervating nerves during postnatal development of mouse lungs.[2] Employing a previously characterized *SMA-GFP;NG2-DsRed* mice that permit separation of ASM from vascular smooth muscle, GFP^+ ASM cells were isolated at postnatal day 21 (P21) after mice were subjected to OVA sensitization and challenge (**Figure 2a**).[22] Comparison of *NT4* mRNA levels in purified ASM cells yielded no significant difference between phosphate-buffered saline (PBS) and OVA exposure (**Figure 2b**). Therefore, ASM is unlikely to be the source of elevated NT4 after OVA exposure in neonatal mice.

We next took an unbiased approach to narrow down candidate cell types that overexpressed NT4 after OVA exposure in neonatal mice. For this, P21 lungs were enzymatically dissociated to yield single-cell suspension followed by cell sorting into three major groups, $CD45^+$ immune cells (including mast cells), $CD31^+$ endothelial cells, and $CD45^-$; $CD31^-$ population (including ASM cells). We found that the only group of cells that had increased *NT4* mRNA levels after OVA exposure was $CD45^+$ immune cells (**Figure 2b**). This finding was consistent with a lack of change in *NT4* gene expression in ASM, a constituent of the $CD45^-$;$CD31^-$ population (**Figure 2b**).

Double staining of mouse lung sections at P21 using an antibody against tryptase, a specific marker of mast cells and the TuJ1 antibody showed that mast cells were often in close proximity to the innervating nerves in airways (**Figure 2c**).[19] In addition, rat peritoneal mast cells were shown to express NTs.[20] To test whether pulmonary mast cells and possibly other immune cell types express NT4, we stained dissociated lung cells for CD45, NT4, and mast cell-specific surface markers, c-kit (CD117), and FcεRI followed by flow cytometry. To ensure specific NT4 labeling, cells from $NT4^{-/-}$ mice were used for gating control (**Figure 2d**). $CD45^+$ immune cells accounted for ~25% total cell population of both wild-type and $NT4^{-/-}$ lungs at P21 (**Figure 2d**). Among these immune cells, 3.09% cells were found to be $NT4^+$ and most of them (90.1%) expressed c-kit (CD117) and FcεRI (**Figure 2d**), indicating NT4 was almost exclusively expressed by pulmonary mast cells within the immune cell population. To confirm this, we performed immunocytochemistry for NT4 using bronchoalveolar lavage collected from OVA-exposed mouse lungs at P21. NT4 was detected in a small percentage of cells with two distinct staining patterns (**Figure 2e**). The punctated and

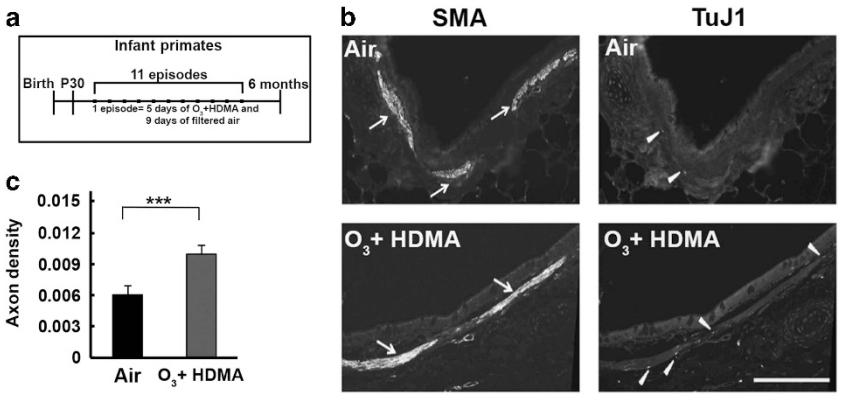

Figure 1 Early-life O_3 and allergen exposure increases airway innervation in nonhuman primate lungs. (**a**) Experimental scheme of O_3 and HDMA exposure in infant nonhuman primates. Controls were exposed to filtered air. (**b**) Assessment of ASM innervation by TuJ1 and alpha-SMA double staining of proximal lung sections from control and O_3 + HDMA-exposed infant rhesus monkeys at 6 months. Arrows indicate ASM and arrowheads indicate innervating nerves. Scale bar, 100 μm. (**c**) Quantification of axon density in ASM of the lungs exposed to filtered air and O_3 + HDMA. Axonal density was measured by normalizing the TuJ1 immunoreactivity to SMA-positive area. A total of 25 sections, 5 from each infant rhesus monkey lung, were quantified. Data represent the mean and s.e.m. $^{***}P < 0.001$.

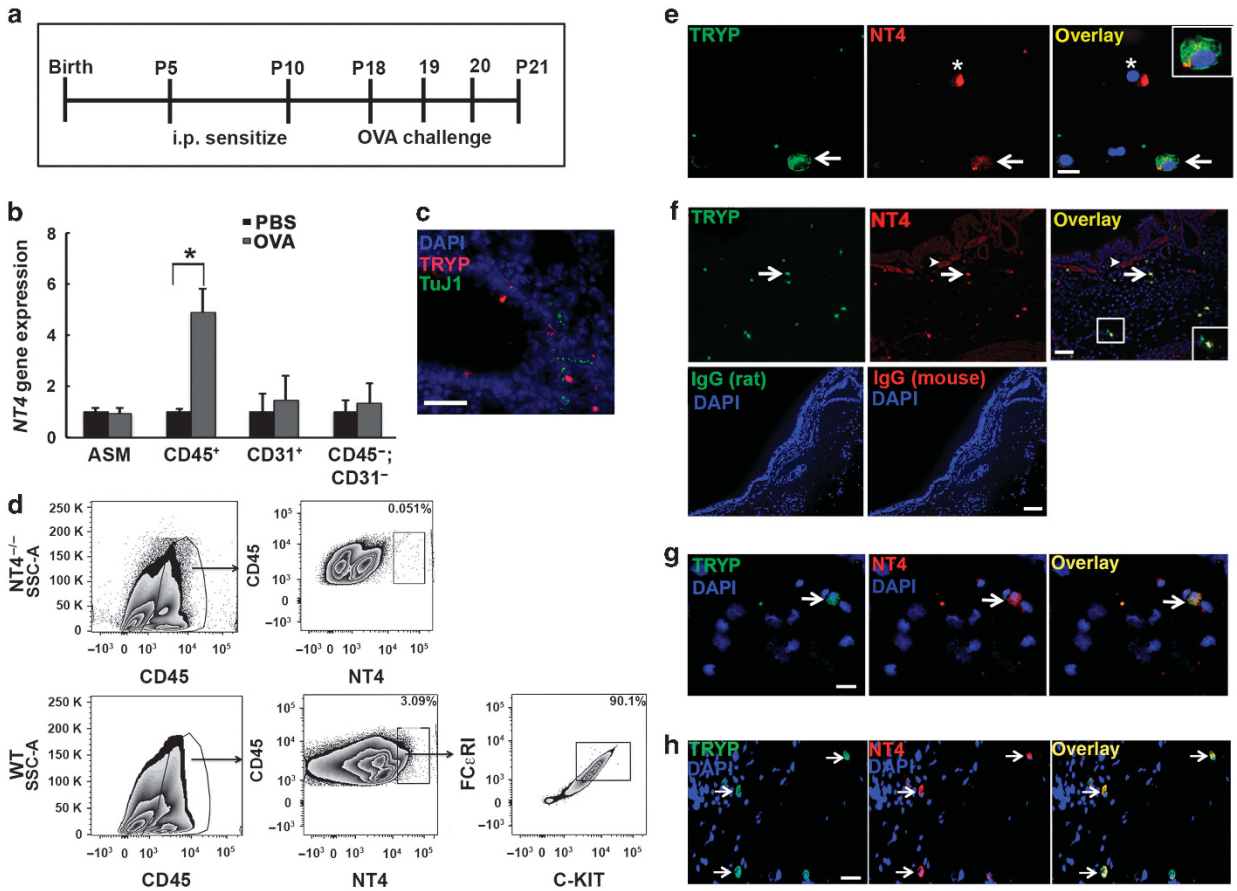

Figure 2 Mast cells are a candidate source of increased NT4 levels in the lung after early-life allergen exposure. (**a**) Experimental protocol of OVA sensitization and challenge in neonatal mice. Controls received PBS challenges. (**b**) Comparison of *NT4* gene expression in ASM and three major cell groups sorted from the lungs of PBS- and OVA-exposed mice at P21. ASM cells were isolated from *SMA-GFP;NG2-dsRed* mice and were pooled from 5–6 mouse lungs as one sample. $N = 3$. (**c**) Double staining for mast cells (red) and nerves (green) in mouse lungs at P21 using a tryptase antibody and the TuJ1 antibody. Scale bar, 50 μm. (**d**) Expression of NT4 in lung immune cells. $CD45^+$ immune cells were gated for NT4 using $NT4^{-/-}$ cells as negative control. $NT4^+$ immune cells were then gated for c-kit and FcεRI. (**e**) Double staining of the immune cells in BAL for NT4 and tryptase. BAL was collected from OVA-exposed mice at P21. The arrow indicates the double-positive cells. * indicates a cell (likely macrophage) with polarized NT4 staining. Insert shows an enlarge image of a double positive mast cell. Scale bar, 25 μm. (**f**) NT4 and tryptase double staining of 6-month-old rhesus monkey lungs. Arrows indicate double-positive mast cells. Arrowheads indicate NT4 expression in ASM. The IgG isotype controls showed no staining. Insert shows an enlarge image of a double positive mast cell. Scale bar, 50 μm. (**g**) Double staining of the cells in endotracheal aspirates from respiratory virus-infected children for NT4 and tryptase. Arrow indicates the double-positive cell. Scale bar, 25 μm. (**h**) Double staining of adult human lung sections for NT4 and tryptase. Arrow indicates double-positive mast cells. Scale bar, 50 μm. Nuclei were stained by DAPI in all images.

diffusive cytoplasmic pattern of NT4 was confirmed to be the secretory granules of mast cells by double staining for tryptase (**Figure 2e**). Very few other cells with a polarized NT4-staining pattern were likely macrophages that engulfed mast cells (**Figure 2e**). Specificity of the NT4 monoclonal antibody and the tryptase antibody for immunocytochemistry was validated by a lack of staining using immunoglobulin G isotype controls and *NT4*$^{-/-}$ mast cells (**Figures 2f** and **4c**).

To test whether mast cells in primate lungs also express NT4, we characterized NT4 expression in the lungs of control, 6-month-old rhesus monkeys. We found that ASM and tryptase^{+} mast cells are the only two cell types that express NT4 in lungs of nonhuman primates (**Figure 2f**), similar to mice. We also characterized NT4 expression in human lungs by double-staining cells in endotracheal aspirates of respiratory virus-infected children and on tissue sections from adult, healthy donor lungs. All NT4^{+} cells in endotracheal aspirates were positive for tryptase (**Figure 2g**). In addition, besides ASM that expressed NT4 (data not shown), all other NT4^{+} cells were mast cells in human lungs (**Figure 2h**). Together, pulmonary mast cells are the predominant immune cell source of NT4 in mice, nonhuman primates and humans.

Mast cell dynamics after early-life allergen exposure

Mast cells are often found close to nerves (**Figure 2c**). In addition to spatial proximity, we reasoned that in order to serve as a functional source of NT4, the number of pulmonary mast cells, NT4 expression, and changes in ASM innervation would be temporally coordinated during the course of insults. To address this issue, we characterized the correlation between the mast cell number and changes in ASM innervation following allergen sensitization and challenge in neonatal mice. At P15 when serum levels of OVA-specific immunoglobulin E (IgE) were increased after two rounds of sensitization (**Supplementary Figure S1a** online), the number of mast cells within and close to ASM was doubled compared with PBS controls (**Figure 3a,b**).[23] This was associated with an ~80% increase in ASM innervation and NT4 levels (**Supplementary Figure S1b–c**). At P21 after OVA challenges, the number of mast cells increased fourfold compared with PBS controls (**Figure 3c, d**), which was positively correlated with elevated levels of NT4 and lung innervation.[2] In addition, toluidine blue staining showed spewed granules surrounding mast cells in OVA-exposed mouse lungs indicating mast cell degranulation (inserts, **Figure 3a,c**), whereas granules were rarely found outside of mast cells in control lungs (**Figure 3a,c**).

Similar to our findings in mice, O_3 + HDMA exposure in infant nonhuman primates almost doubled the number of tryptase^{+} mast cells in ASM when ASM was hyperinnervated (**Figure 3e,f**). Human asthmatics also have increased infiltration of mast cells into ASM.[15] The positive correlation between the number of mast cells and ASM innervation supports mast cells as a candidate for aberrant NT4 expression and ASM hyperinnervation in mice and nonhuman primates and possibly in humans.

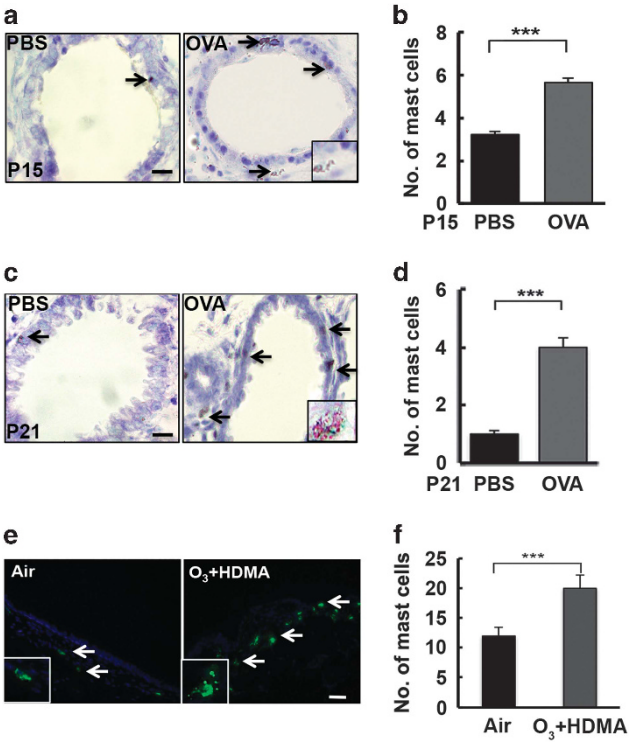

Figure 3 Correlated changes in mast cell number and ASM innervation during early-life insult in mice. Toluidine blue staining and quantification for mast cells in control and OVA-exposed lungs at P15 (**a, b**) and P21 (**c, d**). Arrows point to stained mast cells. Scale bars, 10 μm. Inserts in (**a, c**) provide a zoomed-in view of spewed granules from a mast cell after OVA exposure. Data represent the average and s.e.m. from 10 non-overlapping, 100× images (0.015 mm^2) in mid-lobe sections of each mouse lung and five mice for each condition. *$P<0.05$; ***$P<0.001$. (**e**) Tryptase staining of control and O_3 + HDMA-exposed infant rhesus monkey lungs. Arrows indicate tryptase^{+} mast cells in ASM. Inserts provide a zoomed-in view of tryptase^{+} granules that were mostly inside of a mast cell of control lungs but got spewed from a mast cell in O_3 + HDMA-exposed lungs. Scale bar, 50 μm. (**f**) Quantification of tryptase^{+} mast cells in ASM of control and O_3 + HDMA-exposed infant rhesus monkey lungs. A total of 25 sections from 5 infant monkeys were quantified. Data represent the mean and s.e.m. per 20× field (0.14 mm^2). ***$P<0.001$.

NT4 release requires mast cell degranulation

In allergic asthma, mast cells undergo IgE-mediated degranulation to release several inflammatory mediators.[24] We speculated that NT4 release by degranulation might serve as a mechanism to regulate the bioavailability of NT4 to innervating nerves. To test this hypothesis, we assayed the secretion of NT4 from pulmonary mast cells by cross-linking IgE receptor FcεR1. Primary pulmonary mast cells were obtained after cell suspension from dissociated mouse lungs was treated with stem cell factor and IL-3 over a prolonged period (**Figure 4a**).[25,26] After 3 weeks, the culture was enriched in mature mast cells based on the expression of tryptase and cell surface markers, FcεR1, and c-kit (CD117) that was indistinguishable from an established MC/9 mast cell line (**Figure 4b**). NT4 staining showed that all wild-type primary mast cells expressed NT4, whereas the same mouse monoclonal antibody yielded no positive signal using primary *NT4*$^{-/-}$ mast cells (**Figure 4c**).

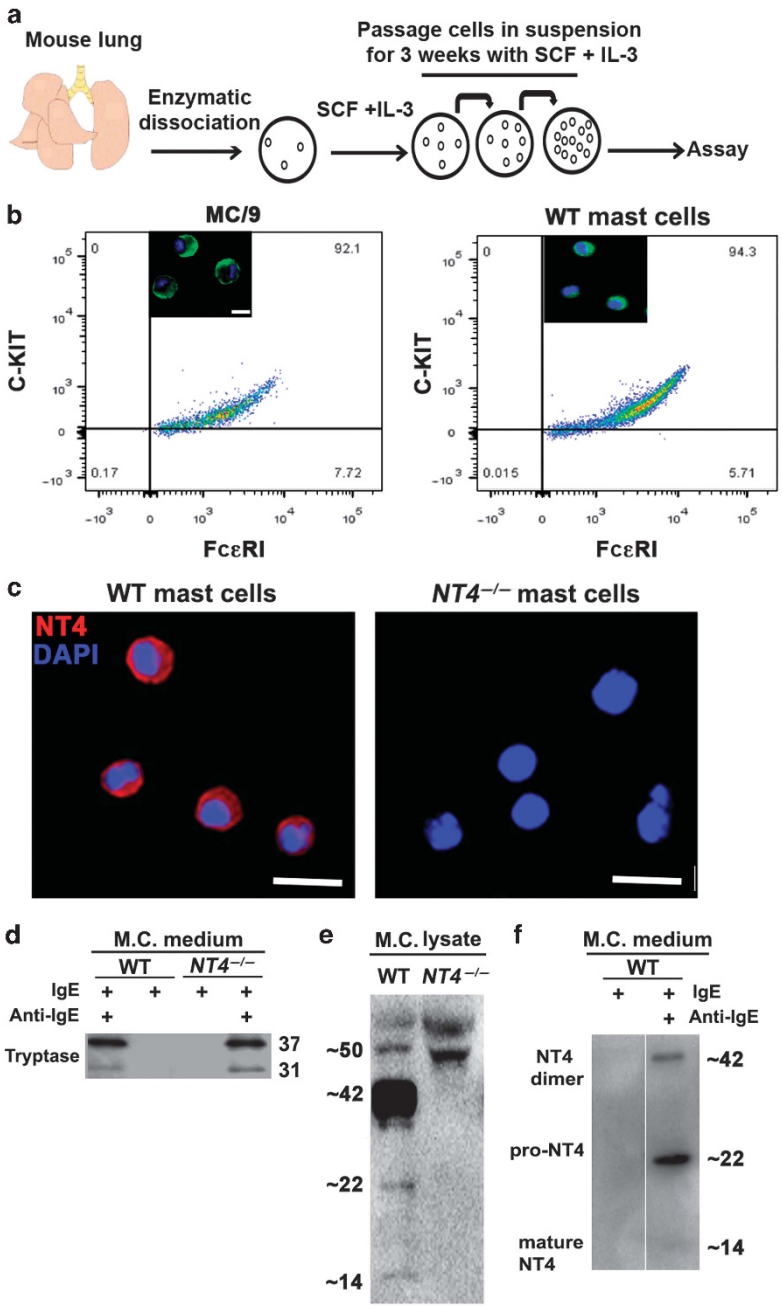

Figure 4 NT4 release requires degranulation of mast cells. (**a**) Experimental protocol of primary pulmonary mast cell culture. (**b**) Flow cytometry analysis of c-kit and FcεR1 expression by primary mast cells and MC/9 mast cells. Inserts showed tryptase staining of cells in culture. (**c**) Staining of primary pulmonary mast cells for NT4. No NT4 staining was detected in *NT4*$^{-/-}$ primary mast cells. Nuclei were stained by DAPI. Scale bar, 10 μm. (**d–f**) Western blot analysis of tryptase and NT4 release in the medium from primary pulmonary mast cells treated with IgE alone (0.5 μg ml^{-1}) or with both IgE and anti-IgE (1 μg ml^{-1}). Data shown represent results from five independent experiments. The specificity of NT4 antibody for western blot analysis was validated (in **e**) using cell lysates of wild-type and *NT4*$^{-/-}$ primary mast cells in culture.

After confirming the purity of primary mast cell cultures, cultures were stimulated with mouse-specific IgE followed by an anti-IgE antibody to induce cross-linking of FcεR1. After 2 h, wild-type and *NT4*$^{-/-}$ primary mast cells degranulated to the same extent assayed by western blot for tryptase released into the media (**Figure 4d**). This indicated that NT4 deficiency does not impact FcεR1-mediated mast cell degranulation. Under the same conditions, NT4 release was assessed using a polyclonal NT4 antibody. The specificity of this polyclonal NT4 antibody was determined by comparing cell lysates of wild-type and *NT4*$^{-/-}$ primary mast cells (**Figure 4e**). The antibody detected specific protein bands representing NT4 in mature form (14 kDa), pro-form (22 kDa), and NT4 dimer (42 kDa) (**Figure 4e**). Other protein bands at higher molecular weight, which were previously reported using rat peritoneal mast cells,[20] were deemed non-specific, as they also appeared in

$NT4^{-/-}$ cell lysates (**Figure 4e**). Guided by these results, we evaluated NT4 in the conditioned media of primary pulmonary mast cell cultures. We did not detect any NT4 under IgE treatment alone (**Figure 4f**). However, upon cross-linking of FcεR1 to induce mast cell degranulation, NT4 in all three forms was released into the media (**Figure 4f**). These findings demonstrate that NT4 release by mast cells is regulated by degranulation. In addition, NT4 itself is not required for degranulation. Consistently, there was no difference in mast cell number and allergen-induced degranulation between wild-type and $NT4^{-/-}$ mice (**Supplementary Figure S2**).

Mast cells are required for allergen-induced ASM hyperinnervation in neonatal mice by releasing NT4

To study the role of pulmonary mast cells in NT4 expression and ASM innervation, we compared NT4 expression and ASM innervation between wild-type and mast cell deficient, $Kit^{W\text{-}sh/W\text{-}sh}$ mice. Unlike other c-kit mutations, $Kit^{W\text{-}sh/W\text{-}sh}$ mice have normal levels of major classes of other differentiated hematopoietic and lymphoid cells.[27–29] After OVA exposure, $Kit^{W\text{-}sh/W\text{-}sh}$ mice exhibited similar levels of inflammation as wild-type mice, assessed by bronchoalveolar lavage counts, serum levels of OVA-specific IgE and the Th2 cytokine IL-13 at P21 (**Figure 5a–c**).[28,29] In addition, we found no change in baseline levels of NT4 protein expression or ASM innervation in $Kit^{W\text{-}sh/W\text{-}sh}$ mice at P21 (**Figure 5d–f**), indicating that mast cells are not required for ASM innervation during development. This is consistent with a lack of NT4 release from mast cells at baseline and provides further evidence in support of ASM-derived NT4 as the target-derived neurotrophic factor for ASM innervation during normal development.[2] Notably, following OVA exposure, $Kit^{W\text{-}sh/W\text{-}sh}$ mice showed no increases in NT4 levels and ASM innervation in contrast to wild-type mice at P21 (**Figure 5d–f**). These findings indicate that c-kit-dependent cell population, which includes mast cells, is required for aberrant NT4 levels and ASM hyperinnervation following early-life allergen exposure in mice. As mast cells are the only other cell type besides ASM that expresses NT4, we speculated that mast cells may become a functional source of NT4 after the expansion of the cell pool and degranulation during insults. In addition, comparing the levels of NT4 between wild-type and $Kit^{W\text{-}sh/W\text{-}sh}$ mice following allergen exposure, activated mast cells may also upregulate NT4 expression.

In addition to mast cell deficiency, $Kit^{W\text{-}sh/W\text{-}sh}$ mice have other non-mast cell-related phenotypes.[27] To definitively prove that mast cells were the functional source of aberrant NT4 levels for ASM hyperinnervation after early-life allergen exposure, we tested whether adoptive transfer of wild-type mast cells, but not $NT4^{-/-}$ mast cells would rescue the phenotypes in OVA-exposed $Kit^{W\text{-}sh/W\text{-}sh}$ mice. After titrating, we determined that 20,000 mast cells via intra-tracheal installation were sufficient to reconstitute the mast cell pool in $Kit^{W\text{-}sh/W\text{-}sh}$ mice to the same levels as in wild-type mice at P21 (**Figure 6a,b**). Wild-type and $NT4^{-/-}$ mast cells were properly located in intra-epithelial and intra-muscular spaces in $Kit^{W\text{-}sh/W\text{-}sh}$ mice after engraftment and spewed out granules upon OVA exposure (**Figure 6b**). Quantification of ASM innervation by TuJ1 staining showed that only wild-type pulmonary mast cells were able to fully restore ASM hyperinnervation in $Kit^{W\text{-}sh/W\text{-}sh}$ mice after OVA exposure, whereas $NT4^{-/-}$ mast cells had no such rescuing activities (**Figure 6c**). Notably, wild-type mast cell reconstitution alone without allergen exposure had no effect on ASM innervation in $Kit^{W\text{-}sh/W\text{-}sh}$ mice (**Figure 6c**), further supporting our finding that NT4 release requires mast cell degranulation (**Figure 4e**).

In addition to quantitative changes, we also evaluated qualitatively whether engraftment of wild-type mast cells restored specific types of innervation in the airway of OVA-exposed $Kit^{W\text{-}sh/W\text{-}sh}$ mice. Lungs were innervated mostly by sensory and parasympathetic nerves.[30] Sensory nerves, labeled by calcitonin gene-related peptide, were found unchanged in wild-type mice following OVA exposure in our previous study.[2] We therefore measured the levels of vesicular acetylcholine transporter (VAChT) in wild-type mice with and without OVA exposure at P21. VAChT is a specific marker of parasympathetic nerves and mediates acetylcholine storage by synaptic vesicles. Compared with saline baseline, allergen exposure led to a fourfold increase in VAChT levels in wild-type mice at P21 assayed by western blot (**Figure 6d**). We then assessed whether engraftment of wild-type mast cells had a similar, inductive effect on parasympathetic lung innervation in $Kit^{W\text{-}sh/W\text{-}sh}$ mice after OVA exposure. Western blot analysis showed that engraftment of wild-type mast cells, but not $NT4^{-/-}$ mast cells, increased the levels of VAChT in OVA-exposed, $Kit^{W\text{-}sh/W\text{-}sh}$ mice by approximately twofold above saline controls (**Figure 6e**). These results indicate an essential role of mast cell-derived NT4 in airway hyperinnervation by cholinergic nerves following allergen exposure.

We previously demonstrated that ASM hyperinnervation following early-life allergen exposure is functionally connected to AHR.[2] To assess AHR in $Kit^{W\text{-}sh/W\text{-}sh}$ mice, we employed precision cut lung slices to measure ASM contraction in response to increasing doses of methacholine (**Figure 6f,g**). Lung slices are largely devoid of humoral factors and free of complications associated with mucus blockade of the airway lumen and therefore, serve as an invaluable assay system for ASM contractility.[31] OVA-exposed $Kit^{W\text{-}sh/W\text{-}sh}$ mice, which had no increase in ASM innervation (**Figure 5e,f**), showed diminished AHR to increasing doses of methacholine compared with OVA-exposed wild-type mice at P21 (**Figure 6f**), consistent with previous reports.[19,32] In addition, $Kit^{W\text{-}sh/W\text{-}sh}$ mice that were engrafted with wild-type pulmonary mast cells, but not $NT4^{-}$ mast cells, recovered AHR to similar levels as wild-type mice following allergen exposure (**Figure 6g**). Together, mast cells functionally contribute to early-life allergen-induced increases in ASM innervation and AHR by releasing NT4 in mice.

DISCUSSION

In this study, we identify a critical role of mast cells in NT4 overproduction, ASM hyperinnervation, and AHR following

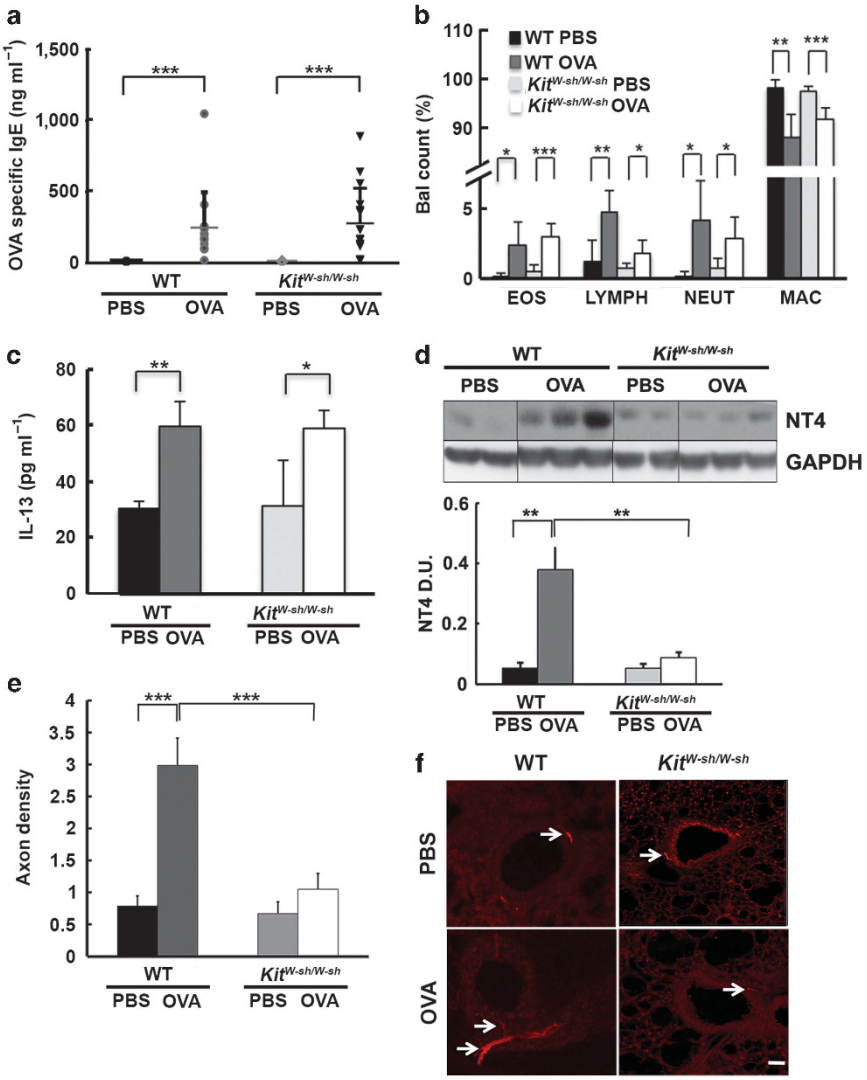

Figure 5 Mast cells are required for increased ASM innervation after early-life OVA exposure in mice. (**a**) Serum levels of OVA-specific IgE in PBS- and OVA-exposed, WT and *Kit*$^{W\text{-}sh/W\text{-}sh}$ mice at P21. $N = 9$. (**b**) Differential BAL count of PBS- and OVA-exposed WT and *Kit*$^{W\text{-}sh/W\text{-}sh}$ mice at P21. The numbers of eosinophils (Eos), lymphocytes (Lymph), neutrophils (Neut), and macrophages (Mac) are shown. $N = 9$. (**c**) Serum levels of IL-13 in PBS- and OVA-exposed WT and *Kit*$^{W\text{-}sh/W\text{-}sh}$ mice at P21 measured by ELISA. $N = 9$. (**d**) Western blot analysis for NT4 protein levels in the lungs of PBS- and OVA-exposed, WT and *Kit*$^{W\text{-}sh/W\text{-}sh}$ mice at P21. Each lane represents one mouse. Glyceraldehyde-3-phosphate dehydrogenase was loading control. Data were normalized to PBS, wild-type control mice. $N = 9$. (**e**) Quantification of the ASM innervation density in control and OVA-exposed, WT and *Kit*$^{W\text{-}sh/W\text{-}sh}$ mice at P21. Data represent the average and s.e.m. from four airways (0.1–0.3 mm^2 in luminal area) of each mouse and 10–12 mice for each condition. (**f**) Representative images of TuJ1 staining of the airway from control and OVA-exposed, WT and *Kit*$^{W\text{-}sh/W\text{-}sh}$ mice at P21. Arrows indicate TuJ1$^+$ axons. Scale bar, 50 μm. $^*P < 0.05$. $^{**}P < 0.01$. $^{***}P < 0.001$.

early-life insult in mice. This role is only evident and essential under pathological conditions and is distinct from inflammatory functions traditionally associated with mast cells during allergic inflammation. In addition to OVA, we showed that repetitive intranasal exposure to cockroach allergen and HDMA similarly caused ASM hyperinnervation in neonatal mice (**Supplementary Figure S3**).[2] These observations indicate that aberrant increases in ASM innervation are generally associated with early-life allergen exposure and are not administration route- or adjuvant-specific. In addition to allergens, O_3 also affects airway innervation in rats following neonatal exposure.[7] In accordance, we showed that exposure to HDMA + O_3 caused an increase in ASM innervation in infant nonhuman primates (**Figure 1**). Although the impact of HDMA and O_3 alone on ASM innervation in infant nonhuman primates warrants future work, we expect that the individual insult may have similar effects on ASM innervation based on previously reported epithelium hyperinnervation following individual or combined insults.[8] Together, building upon our findings in both mice and nonhuman primates, we propose a model for ASM hyperinnervation following early-life insults. In our model, NT4 from ASM serves as an essential trophic factor for innervating nerves that express the NT4 receptor TrkB, thereby establishing ASM innervation during normal

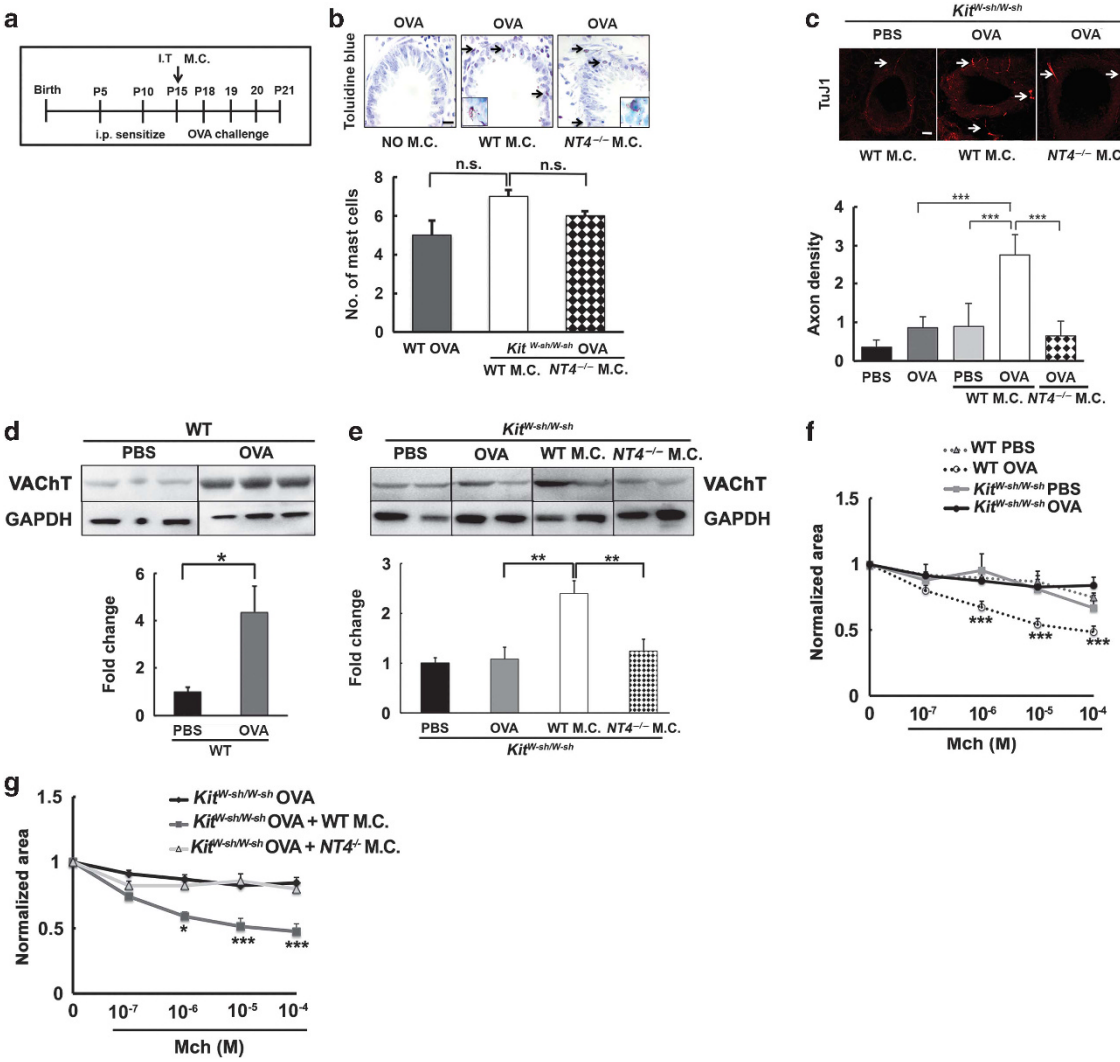

Figure 6 Reconstitution of the mast cell pool in the lungs of $Kit^{W\text{-}sh/W\text{-}sh}$ mice restores early-life allergen-induced increase in ASM innervation and AHR. (**a**) Experimental protocol of adoptive transfer of primary pulmonary mast cells (MC) during OVA exposure. Approximately 20,000 mast cells were installed intratracheally (IT) per mouse at P15. (**b**) Representative images of toluidine blue staining of mast cells in the lungs of $Kit^{W\text{-}sh/W\text{-}sh}$ mice with and without adoptive transfer of mast cells at P21. Arrows indicate pulmonary mast cells in the lung. Scale bar, 10 μm. Inserts showed degranulation of engrafted mast cells. Quantification of mast cells in $Kit^{W\text{-}sh/W\text{-}sh}$ mice after adoptive transfer at P21 was shown in bar graph. Data represent the average and s.e.m. from 10 non-overlapping, 100× images (0.015 mm^2) in mid-lobe sections of each mouse lung and four mice for each condition. (**c**) Representative images of TuJ1 staining of airways (0.1–0.3 mm^2 in luminal area) from PBS- and OVA-exposed $Kit^{W\text{-}sh/W\text{-}sh}$ mice that received intratracheal instillation of WT or $NT4^{-/-}$ pulmonary mast cells. Arrows indicate TuJ1-labeled axons. $N = 6$ mice from three independent experiments. Scale bars, 50 μm. The bar graph shows the quantification of the innervation density of ASM in PBS- and OVA-exposed $Kit^{W\text{-}sh/W\text{-}sh}$ mice with and without adoptive transfer of WT and $NT4^{-/-}$ mast cells. A total of 25 airways from five mice of each group were quantified. Data represent mean ± s.e.m. (**d**) Western blot analysis for cholinergic innervation of the lung at P21. Lung homogenates collected at P21 from PBS- and OVA-exposed wild-type mice were assayed for the levels of VAChT. Each lane represents one mouse. Glyceraldehyde-3-phosphate dehydrogenase was loading control. Data were normalized to PBS control mice. $N = 12$. (**e**) Western blot analysis for cholinergic innervation in lungs of $Kit^{W\text{-}sh/W\text{-}sh}$ mice with and without reconstituted with primary mast cells at P21. Each lane represents one mouse. Glyceraldehyde-3-phosphate dehydrogenase was loading control. $N = 12$. Data were normalized to PBS-exposed $Kit^{W\text{-}sh/W\text{-}sh}$ mice. (**f**) Measurement of airway contraction in response to increasing doses of methacholine using precision cut lung slices from wild-type and $Kit^{W\text{-}sh/W\text{-}sh}$ mice with and without OVA exposure. The size of the airway lumen was normalized to the baseline before methacholine stimulation. Data represented mean ± s.e.m. from 30 airways of three mice for each condition. Two-way ANOVA for multi-variance was used for statistical analysis. Statistically significant differences between WT and $Kit^{W\text{-}sh/W\text{-}sh}$ mice following OVA exposure were marked. (**g**) Measurement of airway contraction in response to increasing doses of methacholine using precision cut lung slices from OVA-exposed $Kit^{W\text{-}sh/W\text{-}sh}$ mice with and without mast cell transfer. Data represented mean ± s.e.m. from 30 airways of three mice for each condition. Statistically significant differences between WT and $NT4^{-/-}$ mast cell transfer were marked. The same results of OVA-exposed $Kit^{W\text{-}sh/W\text{-}sh}$ mice were plotted in both (**f**) and (**g**). $^{*}P < 0.05$; $^{**}P < 0.01$; $^{***}P < 0.001$.

development (**Figure 7**).[2] Following allergen exposure, NT4 expression by ASM is unchanged. However, mast cells increase in number and degranulate to release NT4, thereby becoming a key source of aberrant NT4 expression that in turn causes ASM hyperinnervation and AHR (**Figure 7**). Without mast cells, such as in $Kit^{W\text{-}sh/W\text{-}sh}$ mice, the only cellular source of NT4 in the lung is ASM. As a result, allergen exposure has no effect on ASM innervation and fails to elicit AHR (**Figure 7**). Notably,

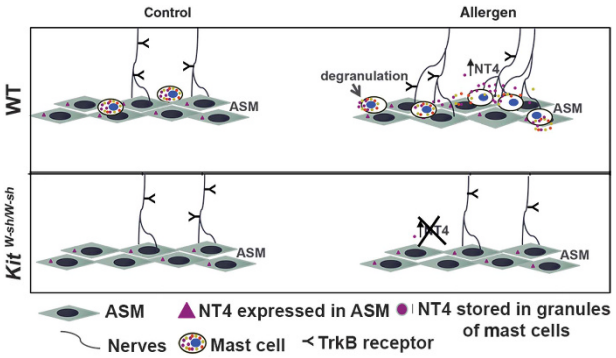

Figure 7 A model of pulmonary mast cells as a key source of elevated NT4 for early-life allergen-induced neuroplasticity. Allergen exposure increases the number of mast cells and triggers degranulation to release NT4, thereby increasing NT4-dependent ASM innervation. This in turn leads to AHR. Without mast cells in the lung, early-life allergen-induced neuroplasticity no longer happens. As a result, there is a lack of AHR in $Kit^{W\text{-}sh/W\text{-}sh}$ mice after early-life allergen exposure.

NT4 expression by ASM and pulmonary mast cells is conserved between mice, nonhuman primates, and humans. In addition, the expansion of the mast cell pool and degranulation similarly occur in rodents, nonhuman primates, and humans in response to a variety of risk factors for asthma. Therefore, mast cells may have a conserved role in ASM hyperinnervation in the infant nonhuman primate model of asthma and thus may contribute to pathogenesis of asthma in human.

In allergic asthma, mast cells are known to degranulate owing to the presence of high levels of IgE in the circulation. IgE-mediated degranulation leads to release of several mediators such as tryptase and NT4 as shown in our study. It is unknown whether these mediators are released simultaneously because they are stored together within the same intracellular granules, or IgE triggers ubiquitous degranulation. Notably, NT4 is secreted in its mature form and pro-form upon IgE-mediated mast cell degranulation. This suggests that the proteolytic process to generate mature NT4 may occur both inside and outside of mast cells by serine proteases and matrix metalloproteinases. Notably, these proteolytic enzymes are abundant during allergic inflammation. Previous studies showed that beta-tryptase from human mast cells cleaved human pro-nerve growth factor to mature nerve growth factor.[33] Whether tryptase is involved in proteolytic maturation of NT4 warrants further study.

The cross-talk between mast cells and nerves contributes to disease pathogenesis in multiple organs. In the lung, mast cells were shown to induce AHR by secreting serotonin to activate the cholinergic nerves in adult mice.[18,19] These previous studies employed $Kit^{W\text{-}sh/W\text{-}sh}$ mice and provided evidence that mast cells have little effects on immune responses to allergen indicating that mast cells are dispensable for allergen-induced airway inflammation in adult mice.[19,28,29] Similarly, our study found little evidence in support of a role of mast cells in allergic inflammation. However, rather than secreting serotonin, our studies in the neonatal mouse model indicate that mast cells communicate with innervating nerves by producing NT4, which leads to ASM hyperinnervation by cholinergic nerves. We provided multiple lines of evidence in support of this unique role of mast cells. First, mast cells are the predominant immune cell type that expresses NT4. Second, mast cell infiltration into ASM increases during repetitive allergen exposure. In addition, NT4 release requires mast cell degranulation. These two features enable mast cells to become a key source of aberrant NT4 levels following insults. Third, the reconstitution experiment in $Kit^{W\text{-}sh/W\text{-}sh}$ mice showed that only wild-type mast cells, but not $NT4^{-/-}$ mast cells, were able to restore ASM hyperinnervation and AHR following insults. These findings rule out the possibility that the phenotypes in allergen-exposed $Kit^{W\text{-}sh/W\text{-}sh}$ mice are caused by non-mast cell defects. Fourth, NT4 deficiency has no effect on the number, differentiation, or degranulation of mast cells (**Supplementary Figure S2**, **Figure 4d**). Last, the relative abundance of mast cells in immature mouse lungs is significantly higher than that in adult mouse lungs. Toluidine blue staining of lung sections showed the density of mast cells is ~20–30-fold higher at P21 than in adult mice at both baseline and after allergen exposure (**Figure 3c,d**, **Supplementary Figure S4**). Consistently, flow cytometry for mast cells using cell surface markers, c-Kit and FCεR1, showed that 0.6–0.9% of all lung cells are mast cells at P21 at the baseline in mice (**Figure 2d**). In comparison, previous studies found only 0.021% of all cells in adult mouse lungs are mast cells.[34] This age-related decrease in the relative abundance of mast cells may explain why mast cells in neonatal lungs have a key role in allergen-induced NT4 overexpression and airway hyperinnervaton, whereas they fail to do so in adult lungs following allergen exposure. These evidences collectively demonstrate a role of mast cell in mediating NT4-induced ASM hyperinnervation following early-life insults. Together, both our study and previous studies highlight the impact of aberrant crosstalk between mast cells and cholinergic nerves on airway reactivity under pathological condition, although the mechanism underlying the cross-talk differs by age.[18,19]

Combining our findings from previous and current studies, mast cell degranulation and NT4 release serve as upstream events that ultimately trigger long-lasting changes in ASM innervation and function following early-life insults. These findings suggest that blockade of mast cell degranulation may be a preventative strategy for young children at high risk of asthma.

METHODS

Mice. Wild-type, $NT4^{-/-}$ (stock number 002497) and $Kit^{W\text{-}sh/W\text{-}sh}$ mice (stock number 012861) were purchased from The Jackson Laboratory. The double fluorescent, *SMA-GFP;NG2-dsRed* mice were described previously.[22] All the mice lines were in C57BL/6 background. All studies with mice were approved by the Institutional Animal Care and Use Committee.

Neonatal mouse model of allergic asthma. Neonatal pups were sensitized and challenged with OVA as described previously.[2] In brief, pups were sensitized at P5 and P10 by intraperitoneal injections of 10 µg OVA (A5503, Sigma, St. Louis, MO) in Imject alum (#7761, Thermo Scientific, Rockford, IL). The sensitized pups were challenged daily with 3% aerosolized OVA solution between P18 and P20. Control pups were challenged with PBS. At day 21, mice were killed for blood,

bronchoalveolar lavage, and lung harvest. Serum levels of OVA-specific IgE and IL-13 were measured with ELISA kits from BioProducts (St. Paul, MN) (M036005) and Life Technologies (Novex, Camarillo, CA) (KMC2221), respectively. bronchoalveolar lavage counts were performed as described.[2]

Fluorescent staining and microscopy. Cells and tissue sections were fluorescently labeled using an established protocol.[2] For endotracheal aspirates from patients at Boston Children's Hospital, the aspirate was treated with collagenase I (10 μg ml^{-1}) for 15 min at 37 °C to degrade the mucus before cells were spun onto a histology slide using Cytospin followed by antibody staining. Primary antibodies include mouse anti-NT4 (1:200, sc-365444, Santa Cruz Biotechnology, Dallas, TX), rat anti-tryptase *β1*/MCPT-7 (1:100, MAB1937, R&D systems, Minneapolis, MN), biotinylated mouse anti-neural class III β-tubulin antibody (TuJ1, 1:200, BAM1195, R&D Systems), and GFP-conjugated mouse anti-SMA antibody (1:500, F3777, Sigma). Isotype controls were rat immunoglobulin G (1:100, ab37361, Abcam, Cambridge, MA) and mouse immunoglobulin G (1:200, sc-2025, Santa Cruz Biotechnology). The biotinylated TuJ1 antibody was detected by streptavidin-Cy3 (1:300, SA1010, Invitrogen, Grand Island, NY). All secondary antibodies were purchased from Life Technologies and included donkey anti-mouse 546 (1:500, A10036), donkey anti-rat 488 (1:500, A21208), and donkey anti-rabbit 546 (1:500, A10040). Fluorescently stained cells and monkey sections were imaged with Axiovert 100M LSM 510 microscope (Zeiss, Peabody, MA). TuJ1 staining of mouse lung slices (100 μm in thickness) was imaged by confocal microscopy. The compressed z-stack images were quantified to determine the innervation density by dividing the TuJ1 immune-reactive area with the perimeter of the airway measured. Airways (0.1–0.3 mm^2 in luminal area) were selected for quantification. For quantification of axon density in rhesus monkey lungs, axon density was calculated by dividing TuJ1-immunoreativity by SMA$^+$ area.

Degranulation assay. Mast cells (2×10^6) were cultured in a 24-well plate in 500 μl of Dulbecco's modified medium. The cells were treated with mouse IgE (0.5 μg ml^{-1}, #553481, BD Biosciences, San Diego, CA) for 2 h at 37 °C. After washing, cells were incubated with anti-mouse IgE (1 μg ml^{-1}, #553413, BD Biosciences) for 2 h at 37 °C. The supernatant was collected before and after anti-IgE treatment. The supernatant was concentrated 10-fold using a spin column with 3 kDa cutoff (#UFC500308, Millipore, Billerica, MA).

Western blot analysis. The protein samples from lungs of P21 mice and lysates/media from mast cell cultures were subjected to western blot analysis described previously.[2] Primary antibodies for VAChT (1:100, Abcam #AB68986) and glyceraldehyde-3-phosphate dehydrogenase (1:10,000, Abcam #AB8245), NT4 (1:100, ANT004, Alomone labs, Jerusalem, Israel) were applied in blocking buffer. The secondary antibodies used were goat anti-rabbit HRP (1:1000, Santa Cruz Biotechnology #sc-2004) and goat anti-mouse HRP (1:5000, BD biosciences #554002). The antigen-antibody complex was detected by SuperSignal West femto Chemiluminescent Substrate (Thermo Scientific). Densitometry units for Individual protein bands were measured using Image J and normalized to its glyceraldehyde-3-phosphate dehydrogenase levels.

Toluidine blue staining for mast cells. Left lung lobes were fixed in 4% paraformaldehyde/PBS at 4 °C overnight. Paraffin sections of 5 μm were stained with 0.1% Toluidine blue (pH 2.0) for 2–3 min after rehydration. The sections were washed by dipping in water 3–5 times followed by dehydration in 100% ethanol. Data were presented as an average of the mast cell number from 10 non-overlapping, 100 × images (0.015 mm^2) in mid-lobe sections for each mouse and 3–5 mice in each condition.

Primary pulmonary mast cell culture. Primary pulmonary mast cells were derived from the lungs of 4-week-old mice following a previously described protocol.[25,26] In brief, lungs were minced, dissociated by collagenase (50 U ml^{-1} in Hanks' balanced salt solution), and filtered through a 40 μm filter. Cells were cultured in Dulbecco's modified medium containing 10% fetal bovine serum, recombinant mouse IL-3 (10 ng ml^{-1}, 213-13; Peprotech, Rocky Hills, NJ), and 10 ng ml^{-1} recombinant stem cell factor (455-MC-010; R&D systems). By the end of 3 weeks, the non-adherent population was enriched in mast cells confirmed using flow cytometric analysis of surface markers, CD117 (1:200, 553869; BD pharmingen, San Diego, CA) and FcεR1 (1:500, 11-5898; eBioscience, San Diego, CA). A MC/9 mast cell line (ATCC CRL-8306) was positive control for flow cytometry.

Adoptive transfer of primary pulmonary mast cells and airway contraction assay. In total, 20,000 mast cells were adoptively transferred into each *Kit$^{W\text{-}sh/W\text{-}sh}$* mouse at P15 via intra-tracheal delivery. These mice were rested for 2 days and followed by OVA challenges. At P21, the lungs were harvested. Precision-cut lung slices (250 μm in thickness) were prepared and assayed similarly as previously described.[2] The airway luminal area was quantified at baseline and after methacholine treatment using Image J. Data were normalized to the pretreatment baseline value.

Cell sorting. Cell suspension and sorting from lungs from *SMA-GFP;NG2-dsRed* mice at P21 were performed as described previously.[22] Antibodies against CD45 (1:100, 30-F11) and CD31 (1:100, MEC 13.3) were purchased from BD Pharmingen. Isotype antibodies were used as controls. Cells were sorted using a Moflo cell sorter (Beckman Coulter, Fullerton, CA). Cells from 5–6 mouse lungs were pooled prior to RNA extraction and gene expression analysis.

Flow cytometry. The lungs were dissociated for cell suspension as described previously.[22] For intracellular staining, the cells were incubated with Golgi Stop (BD biosciences, #554724) for 4 h at 37 °C. Cells were then spun down at 1200 rpm for 5 min and fixed with Cytofix (BD biosciences, #554722) overnight at 4 °C. The next day, the cells were washed with 1 × Perm wash (BD biosciences, #554722) and then stained with the following antibodies: CD45-PERCP.CY5.5 (1:100 BioLegend, San Diego, CA, #103132), CD117- PE (1:200, BD pharmingen553869) and FcεR1-FITC (1:500 eBioscience #11-5898) and NT4-APC (1:50, Santa Cruz Biotech, #sc-365444 special order). Cells were assayed on a FACSCalibur flow cytometer. Data were analyzed using FlowJo software (Tree Star, Ashland, OR).

Statistics. All data are represented as mean ± s.e.m. from a minimum of three separate experiments and each experiment had 3–5 mice per condition Statistical analysis was performed with the two-tailed Student's *t*-test for comparisons between two conditions. For comparison between multiple variances in lung slice contraction assays, data were analyzed with two-way, repeated measures analysis of variance. *P*-value of ≤ 0.05 was considered to be significant.

SUPPLEMENTARY MATERIAL is linked to the online version of the paper at http://www.nature.com/mi

ACKNOWLEDGMENTS

We thank Dr Alan Fine at Boston University School of Medicine for comments and suggestions, Dr Lisa Miller at UC Davis for sending the lung sections of infant rhesus monkeys, Dr Dale Umetsu for assistance with endotracheal aspirate sample collection at Boston Children's Hospital, Juliana Barrios, Kenneth G. Trieu and Dr Yan Bai for technical assistance and critical reading of the manuscript. This work is supported by an American Asthma Foundation award to X. Ai (12- 0086), a NIH grant to B. Levy (R01 HL122531), a NIH grant to L. Miller (P51OD011107) and a T32 training grant to L. Aven (HL007035)

DISCLOSURE

The authors declare no conflict of interest.

REFERENCES

1. Maddox, L. & Schwartz, D.A. The pathophysiology of asthma. *Annu. Rev. Med.* **53**, 477–498 (2002).
2. Aven, L. *et al.* An NT4/TrkB-dependent increase in innervation links early life allergen exposure to persistent airway hyperreactivity. *FASEB J* **28**, 897–907 (2014).
3. Dakhama, A. *et al.* The enhancement or prevention of airway hyper-responsiveness during reinfection with respiratory syncytial virus is critically dependent on the age at first infection and IL-13 production. *J. Immunol.* **175**, 1876–1883 (2005).
4. Stern, D.A., Morgan, W.J., Halonen, M., Wright, A.L. & Martinez, F.D. Wheezing and bronchial hyper-responsiveness in early childhood as predictors of newly diagnosed asthma in early adulthood: a longitudinal birth-cohort study. *Lancet* **372**, 1058–1064 (2008).
5. Gelfand, E.W. Development of asthma is determined by the age-dependent host response to respiratory virus infection: therapeutic implications. *Curr. Opin. Immunol.* **24**, 713–719 (2012).
6. Tan, Y. *et al.* Infection with respiratory syncytial virus alters peptidergic innervation in the lower airways of guinea pigs. *Exp. Physiol.* **93**, 1284–1291 (2008).
7. Hunter, D.D., Wu, Z. & Dey, R.D. Sensory neural responses to ozone exposure during early postnatal development in rat airways. *Am. J. Respir. Cell Mol. Biol.* **43**, 750–757 (2010).
8. Larson, S.D. *et al.* Postnatal remodeling of the neural components of the epithelial-mesenchymal trophic unit in the proximal airways of infant rhesus monkeys exposed to ozone and allergen. *Toxicol. Appl. Pharmacol.* **194**, 211–220 (2004).
9. Yu, M., Zheng, X., Peake, J., Joad, J.P. & Pinkerton, K.E. Perinatal environmental tobacco smoke exposure alters the immune response and airway innervation in infant primates. *J. Allergy Clin. Immunol.* **122**, 640–647 (2008).
10. Wu, Z.X., Hunter, D.D., Kish, V.L., Benders, K.M., Batchelor, T.P. & Dey, R.D. Prenatal and early, but not late, postnatal exposure of mice to sidestream tobacco smoke increases airway hyperresponsiveness later in life. *Environ. Health Perspect.* **117**, 1434–1440 (2009).
11. Huang, E.J. & Reichardt, L.F. Trk receptors: roles in neuronal signal transduction. *Annu. Rev. Biochem.* **72**, 609–642 (2003).
12. Tortorolo, L. *et al.* Neurotrophin overexpression in lower airways of infants with respiratory syncytial virus infection. *Am. J. Respir. Crit. Care Med.* **172**, 233–237 (2005).
13. Szczepankiewicz, A. *et al.* Serum neurotrophin-3 and neurotrophin-4 levels are associated with asthma severity in children. *Eur. Respir. J.* **39**, 1035–1037 (2012).
14. Bauer, O. & Razin, E. Mast-cell nerve interactions. *News Physiol. Sci.* **15**, 213–218 (2000).
15. Brightling, C.E. *et al.* Mast-cell infiltration of airway smooth muscle in asthma. *N. Engl. J. Med.* **346**, 1699–1705 (2002).
16. Van Winkle, L.S., Baker, G.L., Chan, J.K., Schelegle, E.S. & Plopper, C.G. Airway mast cells in a rhesus model of childhood allergic airways disease. *Toxicol. Sci.* **116**, 313–322 (2010).
17. Theoharides, T.C. & Cochrane, D.E. Critical role of mast cells in inflammatory diseases and the effect of acute stress. *J. Neuroimmunol.* **146**, 1–12 (2004).
18. Weigand, L.A., Myers, A.C., Meeker, S. & Undem, B.J. Mast cell-cholinergic nerve interaction in mouse airways. *J. Physiol.* **587**, 3355–3362 (2009).
19. Cyphert, J.M. *et al.* Cooperation between mast cells and neurons is essential for antigen-mediated bronchoconstriction. *J. Immunol.* **182**, 7430–7409 (2009).
20. Skaper, S.D., Pollock, M. & Facci, L. Mast cells differentially express and release active high molecular weight neurotrophins. *Brain Res. Mol. Brain Res.* **97**, 177–185 (2001).
21. Schelegle, E.S. *et al.* Repeated episodes of ozone inhalation amplifies the effects of allergen sensitization and inhalation on airway immune and structural development in Rhesus monkeys. *Toxicol. Appl. Pharmacol.* **191**, 74–85 (2003).
22. Paez-Cortez, J. *et al.* A new approach for the study of lung smooth muscle phenotypes and its application in a murine model of allergic airway inflammation. *PLoS One* **8**, e74469 (2013).
23. Dahlin, J.S., Ivarsson, M.A., Heyman, B. & Hallgren, J. IgE immune complexes stimulate an increase in lung mast cell progenitors in a mouse model of allergic airway inflammation. *PLoS One* **6**, e20261 (2011).
24. Ryan, J.J. *et al.* Mast cell homeostasis: a fundamental aspect of allergic disease. *Crit. Rev. Immunol.* **27**, 15–32 (2007).
25. Tomioka, M., Goto, T., Lee, T.D., Bienenstock, J. & Befus, A.D. Isolation and characterization of lung mast cells from rats with bleomycin-induced pulmonary fibrosis. *Immunology* **66**, 439–444 (1989).
26. Lukacs, N.W. *et al.* The role of stem cell factor (c-kit ligand) and inflammatory cytokines in pulmonary mast cell activation. *Blood* **87**, 2262–2268 (1996).
27. Reber, L.L., Marichal, T. & Galli, S.J. New models for analyzing mast cell functions in vivo. *Trends Immunol.* **33**, 613–625 (2012).
28. Grimbaldeston, M.A., Chen, C.C., Piliponsky, A.M., Tsai, M., Tam, S.Y. & Galli, S.J. Mast cell-deficient W-sash c-kit mutant Kit W-sh/W-sh mice as a model for investigating mast cell biology in vivo. *Am. J. Pathol.* **167**, 835–848 (2005).
29. Becker, M. *et al.* Genetic variation determines mast cell functions in experimental asthma. *J. Immunol.* **186**, 7225–7231 (2011).
30. Aven, L. & Ai, X. Mechanisms of respiratory innervation during embryonic development. *Organogenesis* **9**, 194–198 (2013).
31. Perez, J.F. & Sanderson, M.J. The frequency of calcium oscillation induced 5-HT, ACH and KCl determine the contraction of smooth muscle cells of intrapulmonary bronchioles. *J. Gen. Physiol.* **125**, 535–553 (2005).
32. Yu, M., Tsai, M., Tam, S.Y., Jones, C., Zehnder, J. & Galli, S.J. Mast cells can promote the development of multiple features of chronic asthma in mice. *J. Clin. Invest.* **116**, 1633–1641 (2006).
33. Spinnler, K., Frohlich, T., Arnold, G.J., Kunz, L. & Mayerhofer, A. Human tryptase cleaves pro-nerve growth factor (pro-NGF): hints of local, mast cell-dependent regulation of NGF/pro-NGF action. *J. Biol. Chem.* **286**, 31707–31713 (2011).
34. Li, S. *et al.* Antigen-induced mast cell expansion and bronchoconstriction in a mouse model of asthma. *Am. J. Physiol. Lung Cell Mol. Physiol* **306**, L196–L206 (2014).